Generation of optical vortices in layered helical waveguides

C. N. Alexeyev,* T. A. Fadeyeva, B. P. Lapin, and M. A. Yavorsky
Taurida National V.I. Vernadsky University, Vernadsky Prospekt, 4, Simferopol, 95007, Crimea, Ukraine
(Received 15 January 2011; published 20 June 2011)

We study the possibility of changing the topological charge of incident beams by layered helical structures consisting of planar layers. We show that such structures can effectively change the topological charge of the incoming beam by unity. The problem of the fundamental mode and optical vortex passage through such a layered helical waveguide of a finite length is solved. The spectral characteristics of these processes are obtained. It is shown that such a waveguide can operate as a broadband compact generator of optical vortices from both regular and singular beams.

DOI: 10.1103/PhysRevA.83.063820 PACS number(s): 42.81.Qb

I. INTRODUCTION

The problem of generation of optical vortices (OVs) [1,2]—singularities of phase fronts—has become a classical topic of singular optics. The interest in this problem has been raised due to numerous practical applications of OVs, which encompass such different fields of applied physics as particle trapping [3] and singular beam microscopy [4], micromechanics [5], and astrophysics [6]. Especially promising seems to be the use of OVs as states with a well-defined orbital angular momentum for both classical and quantum information encryption [7] and storage [8]. A number of methods of OV generation have been suggested to date, including generation of vortex beams by lens converters [9], spiral phase plates [10], synthesized holograms [11], and others [12]. Among such methods one can single out a special class, which is connected with the generation of OVs by optical fibers [13]. In this class one of the most elegant methods is concerned with OV generation by helical-core optical fibers. The first experimental demonstration of this phenomenon (without its recognition) dates back to the paper by Poole *et al.*, where they showed mode conversion of the fundamental fiber mode into the field, which is now recognized as the OV [14]. Later on it was shown that such a property of transforming HE_{11} modes into a specific superposition of LP_{01} and LP_{11} modes is inherent in other types of helical fiber gratings [15]. The methods of manufacturing helical-core fibers by drawing from a special perform are promising [16]. A theoretical treatment of this question has been provided in Refs. [17] and [18]. In those papers it has been emphasized that Bragg helical gratings created in fibers render them unique properties concerned with OV guidance.

Whereas it is quite understandable how to produce long-period helical fiber gratings (LPHFGs), it is not clear whether it is possible to create a helical Bragg grating in the fiber. Theoretical models of such gratings implied in Refs. [17] and [18] seem to be quite speculative and abstract. In that regard it is desirable to study more realistic models of engineered helical fiber structures, which could be based on possibilities provided by modern state-of-the-art nanoengineering. It seems natural in this connection to rely on ideas put forward in the field of thin-film sculpturing [19,20]. Recent papers report very impressive results on the fabrication of artificial chiral media [21–23], which draw increasing amounts of attention from both theoreticians and experimenters [24,25].

In this paper we study the property of a chiral structure that consists of planar layers to generate OVs from regular beams. The refractive-index distribution in a layer is assumed to possess axial symmetry and is maximal in the central point. If the structure is built of such identical layers and the central points lay on a regular helix, such a structure may possess pronounced waveguiding properties. In this case one could speak of it as a layered helical waveguide.

The first aim of our paper is to study the possibility of conversion of the fundamental mode into an OV in such a layered structure. We show that in this case the specific way of producing a long-period grating does not affect the ability of layered waveguides to alter the topological charge of the incoming field. We also obtain the spectral characteristics of generators of OVs based on layered helical waveguides, which constitutes the second aim of the present paper. One should emphasize that in our earlier paper [18] we solved only the problem of a HE_{11} mode to vortex conversion in an infinitely long fiber. Solving a realistic problem of fundamental mode passage through a layered helical waveguide of a finite length, we show that such a thin-film waveguide can operate as a broadband OV generator.

II. THE MODEL AND BASIC EQUATIONS

In a layered structure the distribution of the refractive index is given in the most general form as $n(x'(z),y'(z))$, where (x',y') are the Cartesian coordinates introduced in a layer and z is the vertical coordinate of the layer. Let us assume that in the layer n is described by an axially symmetric function $\tilde{n}$: $n(x',y') = \tilde{n}(r')$, where $r'^2 = x'^2 + y'^2$. The location of origin $r' = 0$ is engineered, and in case the origins form the helical curve, one can speak of a layered helical structure. If $\tilde{n}$ is maximal at $r' = 0$ the obtained structure may possess waveguiding properties. Figure 1 illustrates the step-index layered helical waveguide. As can be easily shown, in the global Cartesian frame (x,y,z) the refractive index reads as

$$n(x,y,z) = n(r') \equiv \tilde{n}(\sqrt{r^2 + R^2 - 2rR\cos(\varphi - qz)}), \quad (1)$$

where R is the offset, $q = 2\pi/H$, H is the pitch of helix, and cylindrical-polar coordinates (r,φ,z) connected with the global Cartesian frame are implied. After an evident change of

*Corresponding author: c.alexeyev@yandex.ua

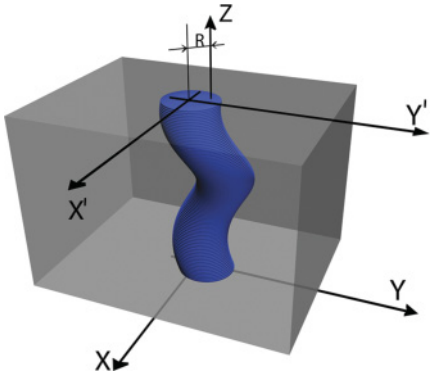

FIG. 1. (Color online) Schematic view of a layered helical waveguide and orientation of global (XYZ) and local ($X'Y'Z'$) Cartesian coordinate frames.

variables $\tilde{r} = r$, $\tilde{z} = z$, $\tilde{\varphi} = \varphi - qz$, one can bring the scalar wave equation that describes propagation of light in such a layered waveguide to the form

$$\left\{\frac{\partial^2}{\partial\tilde{r}^2} + \frac{1}{\tilde{r}}\frac{\partial}{\partial\tilde{r}} + \frac{1}{\tilde{r}^2}\frac{\partial^2}{\partial\tilde{\varphi}^2} + \left(\frac{\partial}{\partial\tilde{z}} - q\frac{\partial}{\partial\tilde{\varphi}}\right)^2 + k^2\tilde{n}^2(\sqrt{\tilde{r}^2 + R^2 - 2\tilde{r}R\cos\tilde{\varphi}})\right\}\vec{E}_t(\tilde{r},\tilde{\varphi},\tilde{z}) = 0, \quad (2)$$

where $\vec{E}_t$ is the transverse electric field, and k is the wave number in vacuum. In what follows we will assume that $R \ll r_0$, where r_0 is the scale of transverse variations of the refractive index. For a step-index structure r_0 can be associated with the core's radius. This assumption enables one to simplify the expression for r', $r' \approx \tilde{r} - R\cos\tilde{\varphi}$, which leads to the following refractive-index distribution:

$$n^2(r,\tilde{\varphi}) \approx n_{co}^2[1 - 2\Delta f(r)] + 2\Delta f_r' R\cos\tilde{\varphi}. \quad (3)$$

Here n_{co} is the refractive index at $r' = 0$, f is some profile function, and Δ is the refractive-index contrast in the transverse plane (cf. notations used in Ref. [26]). In the following we will omit the tilde over r since $r = \tilde{r}$. Since Eq. (2) is translation invariant in z, one can use the standard representation $\vec{E}_t = \vec{e}_t(r,\tilde{\varphi})\exp(i\beta\tilde{z})$, where β is some propagation constant. This leads to the following equation, which is completely analogous to Eq. (6) obtained in Ref. [17]:

$$\left\{\frac{\partial^2}{\partial r^2} + \frac{1}{r}\frac{\partial}{\partial r} + \frac{1}{r^2}\frac{\partial^2}{\partial\tilde{\varphi}^2} + \left(i\beta - q\frac{\partial}{\partial\tilde{\varphi}}\right)^2 + k^2\tilde{n}^2(r) + 2k^2n_{co}^2\Delta f_r' R\cos\tilde{\varphi}\right\}\vec{e}_t(r,\tilde{\varphi}) = 0. \quad (4)$$

At $R = 0$, $q = 0$, this equation describes propagation of light in an effective straight waveguide (see Ref. [26]), whose modes can be written in the basis of linear polarizations [27] $|e\rangle = \binom{e_x}{e_y}$ as

$$|\sigma,l\rangle = \begin{pmatrix}1\\ i\sigma\end{pmatrix}\exp(il\tilde{\varphi})F_l(r), \quad (5)$$

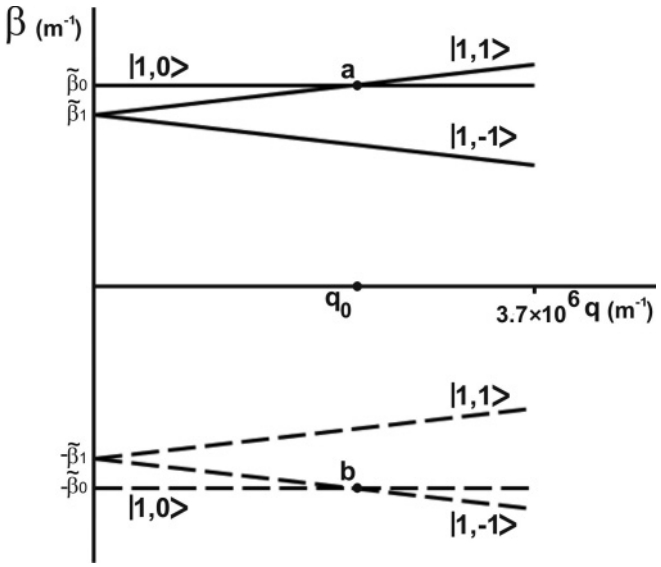

FIG. 2. Zero-approximation spectra of eigenmodes of the matrix $\hat{H}_1(A = 0)$ as functions of the grating parameter q; $q_0 = 5355.75\ \mathrm{m}^{-1}$. The type of mode is indicated over the spectral curve. Note that all the eigenmodes have the same polarization.

where $\sigma = \pm 1$, $l = 0, \pm 1, \pm 2, \ldots$, and F_l satisfies the standard equation in the radial function [26]. Propagation constants of such zero-approximation modes are denoted as $\tilde{\beta}_l$. To study intermodal coupling between $|l| \equiv \ell = 1$ OVs and fundamental modes, one can average Eq. (4) over the basis of the six vectors in Eq. (5) that belong to the $\ell = 0$ and $\ell = 1$ sets [27]: $\{|1,0\rangle,|1,1\rangle,|1,-1\rangle\} \oplus \{|-1,0\rangle,|-1,-1\rangle,|-1,1\rangle\}$. The averaging is carried out according to the standard rule [17,27]. Then the structure of coupled $\ell = 0,1$ modes is defined through the solutions of the eigenvector equation $\hat{H}\vec{x} = 0$, where $\vec{x}$ is a vector defined in a six-dimensional space of $\ell = 0,1$ zero-approximation modes and $\hat{H} = \hat{H}_1 \oplus \hat{H}_2$, where

$$\hat{H}_1 = \hat{H}_2 = \begin{pmatrix}\tilde{\beta}_0^2 - \beta^2 & A & A\\ A & \tilde{\beta}_1^2 - (\beta - q)^2 & 0\\ A & 0 & \tilde{\beta}_1^2 - (\beta + q)^2\end{pmatrix}. \quad (6)$$

For steplike dependence of the refractive index one has (see also Ref. [17]) $A = (\frac{\Delta k^2 n_{co}^2 F_0 F_1}{N_0 N_1}\frac{R}{r_0})_{\rho=1}$, $N_i = \sqrt{\int x F_i^2 dx}$, where $\rho = r/r_0$. The spectrum of modes in a zero approximation reads as $\beta_{1,2} = \pm\tilde{\beta}_0$, $\beta_{3,4} = \pm\tilde{\beta}_1 + q$, $\beta_{5,6} = \pm\tilde{\beta}_1 - q$, and is presented in Fig. 2.

As follows from the results of Refs. [17] and [18], in the points where the zero-approximation spectrum curves intersect, there takes place intensive coupling between forward- or backward-propagating $\ell = 0$ and $\ell = 1$ modes. Such are the points (a) (see Fig. 2), where the coupling of forward-propagating zero-approximation modes takes place, and (b) where backward-propagating modes get coupled. The grating parameter q in these points satisfies the resonance condition $q = q_0 \equiv \tilde{\beta}_0 - \tilde{\beta}_1$. In the vicinity of q_0 the structure of coupled

modes is given by the following expressions:

$$
\begin{aligned}
|\Psi_{1a}\rangle &= \{\cos\chi|1,0\rangle\exp[i(\tilde{\beta}_0+0.5\varepsilon)z]+\sin\chi|1,1\rangle \\
&\quad\times\exp[i(\tilde{\beta}_1-0.5\varepsilon)z]\}\exp\left(\frac{iz}{2}\sqrt{\varepsilon^2+Q^2}\right), \\
|\Psi_{2a}\rangle &= \{-\sin\chi|1,0\rangle\exp[i(\tilde{\beta}_0+0.5\varepsilon)z]+\cos\chi|1,1\rangle \\
&\quad\times\exp[i(\tilde{\beta}_1-0.5\varepsilon)z]\}\exp\left(-\frac{iz}{2}\sqrt{\varepsilon^2+Q^2}\right), \\
|\Psi_{3b}\rangle &= \{-\sin\chi|1,0\rangle\exp[-i(\tilde{\beta}_0+0.5\varepsilon)z]+\cos\chi|1,-1\rangle \\
&\quad\times\exp[-i(\tilde{\beta}_1-0.5\varepsilon)z]\}\exp\left(\frac{iz}{2}\sqrt{\varepsilon^2+Q^2}\right), \\
|\Psi_{4b}\rangle &= \{\cos\chi|1,0\rangle\exp[-i(\tilde{\beta}_0+0.5\varepsilon)z]+\sin\chi|1,-1\rangle \\
&\quad\times\exp[-i(\tilde{\beta}_1-0.5\varepsilon)z]\}\exp\left(-\frac{iz}{2}\sqrt{\varepsilon^2+Q^2}\right),
\end{aligned}
\tag{7}
$$

where $\varepsilon = q - q_0$, $\tan\chi = Q/(\sqrt{\varepsilon^2+Q^2}-\varepsilon)$, $Q \approx A/\tilde{\beta}_0$, and $\chi \in [\frac{\pi}{4},\frac{\pi}{2}]$. Note that the modes $|\Psi_{3,4b}\rangle$ are formed due to coupling of backward-propagating zero-approximation modes. Equations (7) are sufficient to describe mode conversion in layered helical waveguides.

III. GENERATION OF OPTICAL VORTICES IN LAYERED WAVEGUIDES

Near the resonance point, due to a strong coupling between forward-propagating $\ell = 0,1$ modes, helical core fibers may change the topological charge of the incoming field. Using the results of Ref. [18], one can demonstrate that if at the input end of an infinitely long helical core fiber one excites the fundamental mode $|1,0\rangle$, it evolves in the fiber as

$$
\begin{aligned}
|\Phi(z)\rangle = \Bigg\{\Bigg[\cos(0.5z\sqrt{\varepsilon^2+Q^2}) &+ \frac{i\varepsilon}{\sqrt{\varepsilon^2+Q^2}} \\
\times\sin(0.5z\sqrt{\varepsilon^2+Q^2})\Bigg]|1,0\rangle &+ \frac{iQ}{\sqrt{\varepsilon^2+Q^2}} \\
\times\sin(0.5z\sqrt{\varepsilon^2+Q^2})|1,1\rangle\Bigg\}&\exp[i(\tilde{\beta}_1+0.5\varepsilon)z].
\end{aligned}
\tag{8}
$$

A complete transformation of the $|1,0\rangle$ mode into the $|1,1\rangle$ OV is possible only at a zero detuning, $\varepsilon = 0$. As is evident, at

$$
z = S_m = \frac{(2m-1)\pi}{Q}, \tag{9}
$$

where $m = 1,2,\ldots$, the cosine term vanishes and the resulting field is represented by an OV of topological charge 1, $|\Phi(S_m)\rangle \propto |1,1\rangle$. The last relation conveys the conversion of the fundamental mode into the OV. Typical values of conversion length in infinite fibers are of 10^{-3} m order. For example, for a fiber with parameters $V = 5.96$, $r_0 = 10\lambda$, $R/r_0 = 0.1$, $n_{co} = 1.5$, $\Delta = 0.002$ at wavelength $\lambda = 0.6328\times10^{-6}$ m, the length of conversion $|1,0\rangle \to |1,1\rangle$ is $\tilde{S}_1 = 0.0016$ m. This length can be diminished by increasing the optical contrast (the value of Δ) or by increasing the ratio R/r_0. It is natural to set the fiber's length d to S_m while studying the realistic problem

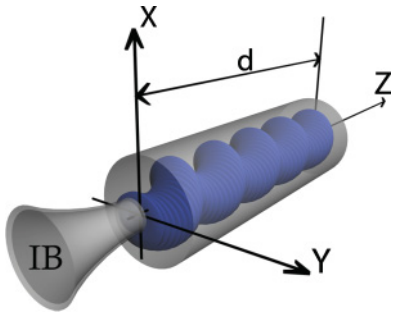

FIG. 3. (Color online) Orientation of the coordinate frame in the problem of passage of an incident light beam (IB) through a section of a layered helical waveguide of length d.

of OV generation by a finite-length fiber. The geometry of the problem is shown in Fig. 3.

Following Ref. [28], consider the problem of excitation of the helical layered fiber with the fundamental-like Gaussian mode, which at the condition of waist size matching [26] can be approximated by the $|1,0\rangle$ vector. Then in the left half-space the field can be represented in the form

$$
\begin{aligned}
|\Phi_1(z\leqslant 0)\rangle = |1,0\rangle e^{ikz} + R_1|1,0\rangle e^{-ikz} + R_2|1,1\rangle e^{-ikz} \\
+ R_3|1,-1\rangle e^{-ikz}.
\end{aligned}
\tag{10}
$$

Here we have taken into account that, due to topological activity of the helical fiber, the reflected field may also comprise OVs of charge ±1. Note that since the perturbation term in Eq. (4) does not couple the states with different polarizations, no leftcircularly polarized components are present in the reflected field.

The field within the fiber is given by

$$
\begin{aligned}
|\Phi_2(0\leqslant z\leqslant d)\rangle = T_1|\psi_{1a}\rangle + T_2|\psi_{2a}\rangle + T_3|\psi_{3b}\rangle + T_4|\psi_{4b}\rangle \\
+ T_5|1,1\rangle e^{-i\tilde{\beta}_1 z} + T_6|1,-1\rangle e^{i\tilde{\beta}_1 z}.
\end{aligned}
\tag{11}
$$

On the right-hand side of the fiber the field will be represented as

$$
|\Phi_3(z\geqslant d)\rangle = (P_1|1,0\rangle + P_2|1,1\rangle + P_3|1,-1\rangle)e^{ik(z-d)}. \tag{12}
$$

Here R_i, T_i, and P_i are the unknown coefficients. Matching the fields and their derivatives with respect to z enables one to obtain the set of linear algebraic equations in the unknown coefficients. Figure 4 demonstrates the dependence of the transmission coefficient $|P_2|^2$ for OV $|1,1\rangle$ on the wavelength λ of the incoming field for $d = S_1$. As is seen, in this case such a layered structure operates as a broadband generator of OVs. The generation of the OV is accompanied by a simultaneous dip in the transmission coefficient $|P_1|^2$ of the fundamental mode, shown in Fig. 5. As the order m of the conversion length S_m increases, the transmission curve for $|P_2|^2$ features a number of peaks located at different wavelengths (see Fig. 6). Simultaneously, the width of the peaks decreases.

As is evident, the curves in Figs. 4–6 feature the presence of two strongly differing scales of variation with wavelength. This is connected with the presence of two scales in coefficients, which determine the set of equations in reflection and transmission coefficients. Indeed, matching the fields at

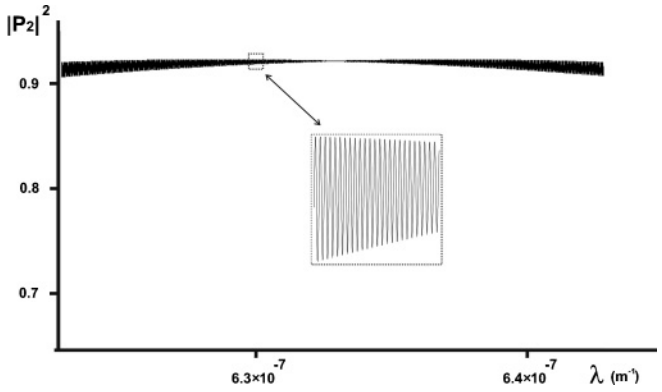

FIG. 4. The dependence of the transmission coefficient $|P_2|^2$ for OV $|1,1\rangle$ on the wavelength λ of the incoming field at the fiber's length $d = S_1 = 0.0033$ m, central wavelength $\lambda_0 = 0.6328 \times 10^{-6}$ m, $V = 5.96$, $r_0 = 10\lambda_0$, $R/r_0 = 0.1$, $n_{co} = 1.5$, and $\Delta = 0.002$.

the right-hand boundary of the fiber leads to the appearance of factors $\exp(i\tilde{\beta}_l d)$ and $\exp(-\frac{id}{2}\sqrt{\varepsilon^2 + Q^2})$ [see Eq. (7)] in the structure of such coefficients. Using the approximation $\tilde{\beta}_l \approx 2\pi n_{co}/\lambda$, one can readily obtain the decomposition of this factor near some central wavelength λ_0 in the form $\exp[i\tilde{\beta}_l(\lambda_0)d(1 + \frac{\Delta\lambda}{\lambda_0})]$, where $\Delta\lambda = \lambda - \lambda_0$, which leads to oscillations on the scale $\Lambda_1 = \frac{\lambda_0}{\tilde{\beta}_l(\lambda_0)d}$. Since in our case $\tilde{\beta}_l d \gg 1$ (as a matter of fact, it has the order of 10^3–10^4 at $d = S_1$) essential variations of this factor takes place even at $\Delta\lambda = 10^{-3}\lambda_0$–$10^{-4}\lambda_0$, which explains the presence of a superfine structure of transmission and reflection curves shown in the insets in Figs. 4–6. This phenomenon is well known in the optics of layered media [29] and is associated with an action of the medium as a whole. For chiral fibers this is also a well-established fact [28].

In the same manner one can explain the presence of larger-scale variations presented in Fig. 6. Although the superfine structure is also present (see the inset), there are large-scale oscillations due to another periodic in $\Delta\lambda$ factor of $\exp(-\frac{id}{2}\sqrt{\varepsilon^2 + Q^2})$, which can be decomposed at $\varepsilon = 0$ as $\exp[-\frac{id}{2}Q(\lambda_0) - \frac{id}{2}Q'(\lambda_0)\Delta\lambda]$. Since $Q'(\lambda_0) \approx -Q(\lambda_0)/\lambda_0$ the scale of variations associated with this term is $\Lambda_2 = \frac{\lambda_0}{Q(\lambda_0)d}$. Due to the inequality $Q/\tilde{\beta}_l \ll 1$, this term appears to be less sensitive to variations of $\Delta\lambda$ than the previously discussed one and is responsible for large-scale oscillations of the transmission coefficient.

Even a superficial comparison with the corresponding result of Ref. [18] reveals that the spectral width of OV generation in a layered helical waveguide is greater than the one for a helical-core fiber. Basically, this is connected with the difference in the ways of creating the helical perturbation of the refractive-index distribution. Whereas in layered waveguides the helical distribution is created by displacement of layers, in helical-core fibers the perturbation term arises due to purely geometric factors. This leads to their different dependence on parameters of the helical grating. In helical-core fibers the perturbation term that provides the coupling of OVs and fundamental modes is proportional to the curvature κ of the central line, $\kappa \approx 4\pi^2 R/H^2$, for long-period gratings. As is evident, the strength of the coupling depends on pitch H and for long-period helical-core fibers it decreases. In contrast, for layered waveguides the perturbation term does not depend on the grating's pitch and in this way ensures more effective coupling of modes, which results in a greater width of transmission curves.

IV. CONVERSION OF HIGHER-ORDER OPTICAL VORTICES

In the same manner one can study the transformation of OVs with higher values of the topological charge. Let us consider the case of mode conversion between charge-1 and charge-2 OVs. To this end one should build the matrix of the total operator $\hat{H}$ on the left-hand side of Eq. (4) on the basis of zero-approximation vectors $\{|1,1\rangle, |1,-1\rangle, |1,2\rangle, |1,-2\rangle\}$ that belong to eigenvalues $\tilde{\beta}_1$ and $\tilde{\beta}_2$. Note that once again these vectors have the same polarization, which reflects separability of the zero-approximation solutions in polarization. The corresponding matrix reads as

$$\tilde{H} = \begin{pmatrix} \tilde{\beta}_1^2 - (\beta - q)^2 & 0 & B & 0 \\ 0 & \tilde{\beta}_1^2 - (\beta + q)^2 & 0 & B \\ B & 0 & \tilde{\beta}_2^2 - (\beta - 2q)^2 & 0 \\ 0 & B & 0 & \tilde{\beta}_2^2 - (\beta + 2q)^2 \end{pmatrix}, \tag{13}$$

where the coupling constant is $B = (\frac{\Delta k^2 n_{co}^2 F_1 F_2}{N_1 N_2}\frac{R}{r_0})_{\rho=1}$. Zero-approximation spectra (at $B = 0$) have the form

$$\beta_{1,2} = \pm\tilde{\beta}_1 + q, \quad \beta_{3,4} = \pm\tilde{\beta}_1 - q, \qquad \beta_{5,6} = \pm\tilde{\beta}_2 + 2q, \quad \beta_{7,8} = \pm\tilde{\beta}_2 - 2q. \tag{14}$$

The plots of the spectrum curves are shown in Fig. 7. These curves intersect in the points (a)–(d), where the kinematic resonance conditions are satisfied. In these points the spectral curves may get coupled, which corresponds to resonance coupling of related OVs. However, to ensure such coupling the dynamical condition must also be fulfilled: The corresponding matrix element of the perturbation operator built over those states must be nonzero. Since in our approximation the perturbation term is proportional to $\cos\tilde{\varphi}$, it can couple only the states whose orbital numbers differ by unity. That is why no mode coupling takes place near points (c) and (d): The orbital numbers of OVs, whose spectral curves intersect in those points, differ by 3.

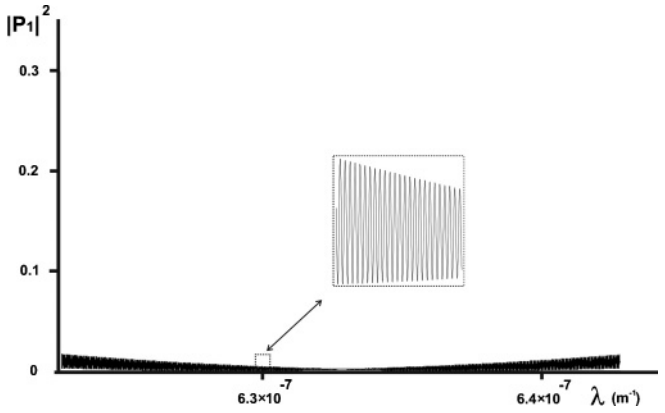

FIG. 5. The dependence of the transmission coefficient $|P_1|^2$ of the fundamental mode $|1,0\rangle$ on the wavelength λ at the fiber's length $d = S_1$, central wavelength $\lambda_0 = 0.6328 \times 10^{-6}$ m, $V = 5.96$, $r_0 = 10\lambda_0$, $R/r_0 = 0.1$, $n_{co} = 1.5$, and $\Delta = 0.002$.

Near points (a) and (b), where the kinematical resonance condition $q = q_1 \equiv \tilde{\beta}_1 - \tilde{\beta}_2$ is fulfilled, the dimension of the eigenvalue equation can be reduced. For example, near (a) one has

$$\begin{pmatrix} \tilde{\beta}_1^2 - (\beta - q)^2 & B \\ B & \tilde{\beta}_2^2 - (\beta - 2q)^2 \end{pmatrix} \vec{x} = 0, \qquad (15)$$

where $\vec{x} = \mathrm{col}(a,b)$ stands for the hybrid mode $a|1,1\rangle + b|1,2\rangle$. The expressions for the coupled modes near points (a) and (b) read as

$$|\psi_{1a}\rangle = \{\cos\chi_2|1,1\rangle \exp[i(\tilde{\beta}_1 + 0.5\varepsilon')z] + \sin\chi_2|1,2\rangle \times \exp[i(\tilde{\beta}_2 - 0.5\varepsilon')z]\} \exp\left(\frac{iz}{2}\sqrt{\varepsilon'^2 + P^2}\right),$$

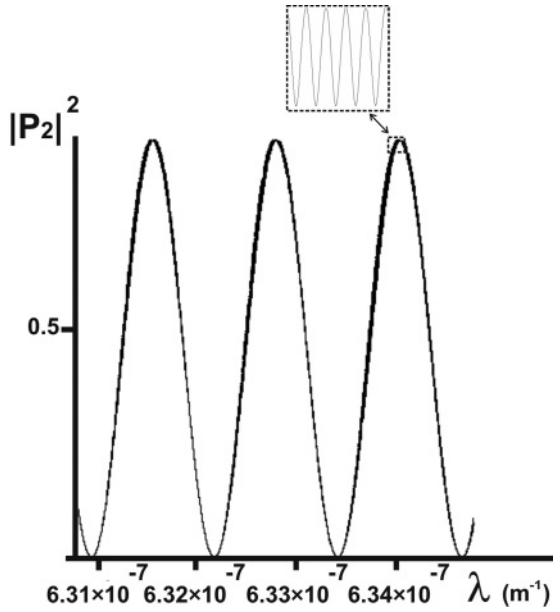

FIG. 6. Transmission coefficient $|P_2|^2$ for OV $|1,1\rangle$ vs wavelength λ at the fiber's length $d = S_{500}$, central wavelength $\lambda_0 = 0.6328 \times 10^{-6}$ m, $V = 5.96$, $r_0 = 10\lambda_0$, $R/r_0 = 0.1$, $n_{co} = 1.5$, and $\Delta = 0.002$.

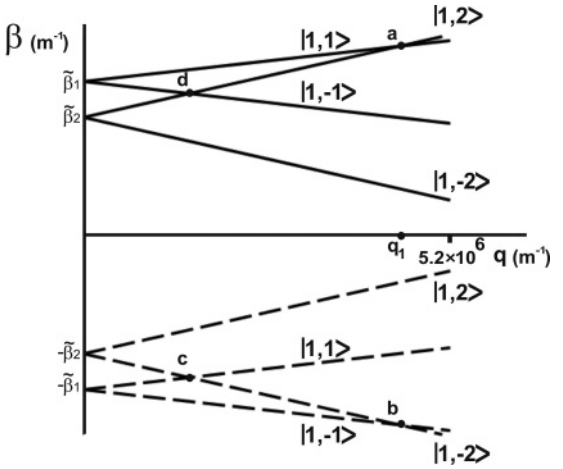

FIG. 7. Zero-approximation spectra of eigenmodes of the matrix $\hat{H}(B = 0)$ as functions of the grating parameter q; $q_1 = 6888.6$ m^{-1}. The type of mode is indicated over the spectral curve.

$$|\psi_{2a}\rangle = \{-\sin\chi_2|1,1\rangle \exp[i(\tilde{\beta}_1 + 0.5\varepsilon')z] + \cos\chi_2|1,2\rangle \times \exp[i(\tilde{\beta}_2 - 0.5\varepsilon')z]\} \exp\left(-\frac{iz}{2}\sqrt{\varepsilon'^2 + P^2}\right), \qquad (16)$$

$$\begin{aligned} |\psi_{1b}\rangle &= \{-\sin\chi_2|1,-1\rangle \exp[-i(\tilde{\beta}_1 + 0.5\varepsilon')z] \\ &\quad + \cos\chi_2|1,-2\rangle \exp[-i(\tilde{\beta}_2 - 0.5\varepsilon')z]\} \\ &\quad \times \exp\left(\frac{iz}{2}\sqrt{\varepsilon'^2 + P^2}\right), \\ |\psi_{2b}\rangle &= \{\cos\chi_2|1,-1\rangle \exp[-i(\tilde{\beta}_1 + 0.5\varepsilon')z] \\ &\quad + \sin\chi_2|1,-2\rangle \exp[-i(\tilde{\beta}_2 - 0.5\varepsilon)z]\} \\ &\quad \times \exp\left(-\frac{iz}{2}\sqrt{\varepsilon'^2 + P^2}\right) \end{aligned} \qquad (17)$$

where $\tan\chi_2 = P/(\sqrt{\varepsilon'^2 + P^2} - \varepsilon')$, $P = B/\tilde{\beta}_1$, $\varepsilon' = q - \tilde{\beta}_1 + \tilde{\beta}_2$, and $\chi_2 \in [\frac{\pi}{4}, \frac{\pi}{2}]$.

In the same manner one can study the resonance conversion of OVs by a segment of such a fiber near the resonance points. For example, if the vortex $|1,1\rangle$ is incident at the input end it gives rise to the following fields outside the fiber and within in

$$\begin{aligned} |\Phi(z \leqslant 0)\rangle &= |1,1\rangle e^{ikz} + R_1|1,1\rangle e^{-ikz} + R_2|1,2\rangle e^{-ikz} \\ &\quad + R_3|1,-1\rangle e^{-ikz} + R_4|1,-2\rangle e^{-ikz}, \\ |\Phi_2(0 \leqslant z \leqslant d)\rangle &= T_1|\psi_{1a}\rangle + T_2|\psi_{2a}\rangle + T_3|\psi_{1b}\rangle + T_4|\psi_{2b}\rangle \\ &\quad + T_5|1,1\rangle e^{-i\tilde{\beta}_1 z} + T_6|1,2\rangle e^{-i\tilde{\beta}_2 z} \\ &\quad + T_7|1,-1\rangle e^{i\tilde{\beta}_1 z} + T_8|1,-2\rangle e^{i\tilde{\beta}_2 z}, \\ |\Phi_3(z \geqslant d)\rangle &= (P_1|1,1\rangle + P_2|1,2\rangle + P_3|1,-1\rangle \\ &\quad + P_4|1,-2\rangle) e^{ik(z-d)}. \end{aligned} \qquad (18)$$

Matching the fields and their derivatives on the boundaries enables one to determine the transition coefficients of constituent OVs. The conversion of OVs in an infinitely long fiber takes place at the distances [18]

$$\tilde{S}_m = \frac{(2m-1)\pi}{P}, \qquad (19)$$

where m is an integer. Analogously, we set $d = \tilde{S}_m$ to study the transmission curves. Figure 8 shows the

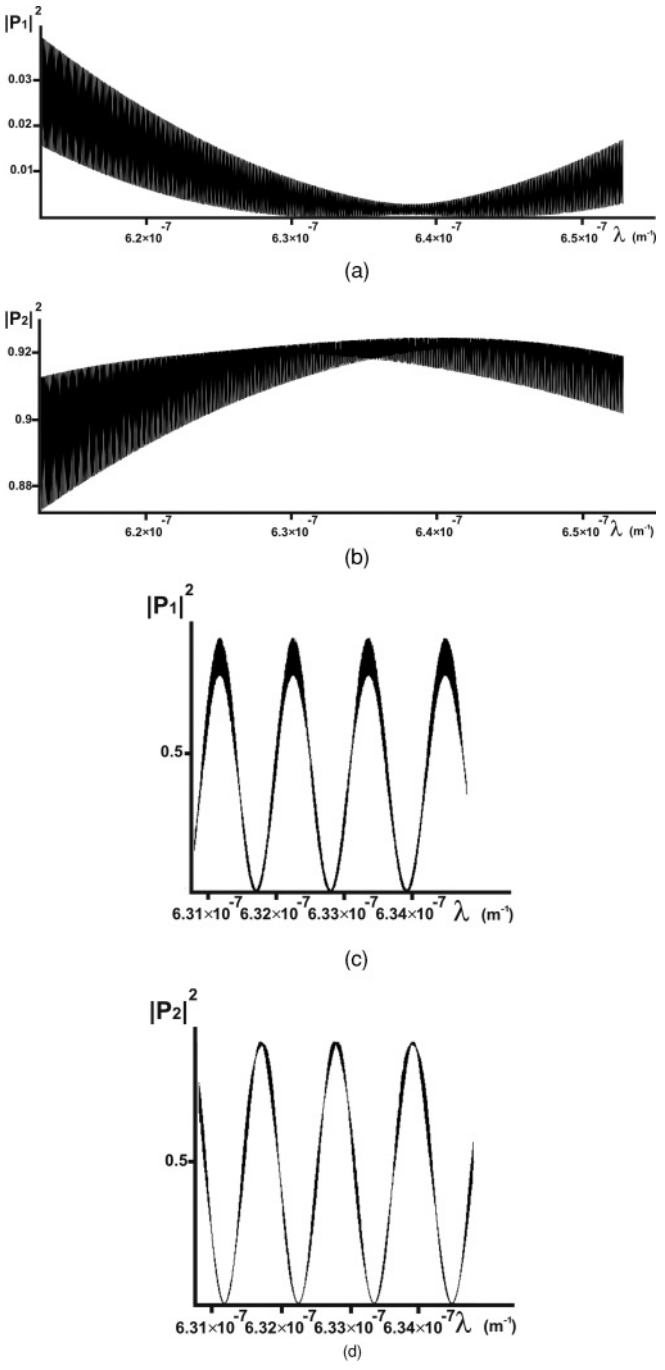

FIG. 8. Transmission coefficients for OVs: (a) $|1,1\rangle$ and (b) $|1,2\rangle$ vs wavelength λ for incident OV $|1,1\rangle$. The fiber's length $d = \tilde{S}_1 = 0.0016$ m, central wavelength $\lambda_0 = 0.6328 \times 10^{-6}$ m, $V = 5.96$, $r_0 = 10\lambda_0$, $R/r_0 = 0.1$, $n_{co} = 1.5$, and $\Delta = 0.002$. (c) and (d) Transmission coefficients for $|1,1\rangle$ and $|1,2\rangle$ OVs, respectively, at $d = \tilde{S}_{500}$.

transmission curves of certain OVs for various fiber lengths.

The examples of transformations of incoming fields given above, which are accompanied by the change in topological charge, show that such a system possesses both the features of broadband transformation and diminutiveness. Indeed, the minimal conversion length S_1 has the order of a millimeter. This could be very important in the creation of miniature devices for topological charge control in communication optics based on information encoding on states with an orbital angular momentum. It should be emphasized that all the existing analogs lack this property. Moreover, there is the potential of further decreasing the longitudinal size of such converters. It is connected with the fact that the kinematical resonance condition $q = q_i$, which sets the lower limit to the grating's pitch, does not pose limitations to the minimal length S_1 (or $\tilde{S}_1$), at which the mode conversion takes place. The latter is rather related to the dynamical resonance conditions Eqs. (9) and (19) that involve the value of the matrix elements and not the difference in scalar propagation constants. In this way it is possible to decrease the minimal conversion length by increasing the mode coupling constants. For example, since the latter depend on an offset to core's radius ratio R/r_0, there is the possibility of controlling the coupling by engineering this geometrical parameter. In numerical simulations we have assumed this ratio to be 0.1. Of course, increasing this ratio may lead to certain radiation losses; however, since in this situation we are not much concerned with effective light guidance, this seems to be a reasonable price for further miniaturization of the device. The availability of such compact OV generators could also be useful while creating arrays of OVs [30].

Finally, let us discuss in brief some questions concerning the practicality of fabricating such layered waveguides and the applicability of the existing methods to their manufacture. As is evident, manufacturing LPHFGs is a much less challenging problem as compared, for example, to the problem of making such structures with a subwavelength pitch. Historically, the first such grating was produced by wiring a two-mode fiber coupler [14]. At present, such structures are made either by releasing the residual stress of a fiber without twisting it by heating it with a CO_2 laser beam [31] or by twisting it with simultaneous heating of the working zone [16,32]. This technique enables one to control the period of the grating, however, it is less efficient in controlling the coupling strength, which depends on the geometry of a lateral cross section of the fiber. Besides, the evolution of the input beam may be strongly complicated by the scattering of the core modes into the cladding modes of the fiber [33].

The required accuracy of manufacturing such gratings can be achieved only with the use of modern nanoengineering techniques. In the past decades several methods have been developed for the fabrication of three-dimensional (3D) photonic structures. Among them are techniques which provide relatively large structures in a parallel configuration: colloidal self-assembly, holographic laser lithography, and phase-mask holography. The creation on a nanoscale of multiple arrayed chiral structures by such techniques has been reported [19]. Although such methods do not allow maintaining the circular form of the individual fiber's cross section, its form is not very relevant for mode conversion. It is more important to control the pitch of a helix. Deviation from the ideal circular form may lead to deterioration of the conversion characteristics and the appearance of other types of "parasitic" conversions into other modes, which is mainly connected with the structure of modes of waveguides with a noncircular cross section. It is not quite clear, though, whether it is possible to fabricate by such methods a solitary helical waveguide. Other methods of

producing arrayed helical structures in sculptured thin films by vapor deposition on a rotating substrate seem to be of less relevance because of an essential difference in scales: The pitch of the helices in such films varies from 20 to 1100 nm [19], whereas the pitch in LPHFGs has to be several hundreds of micrometers.

In view of this, it is more appropriate to suggest using the methods concerned with direct laser writing for fabrication of LPHFGs [21–23,34]. The obtained resolution of 180 nm for extended structures would enable one to maintain the desired accuracy of reproducing the transverse form of the helical layered waveguide. Indeed, for $R/r_0 = 0.1$ and $r_0 = 10\lambda_0$ the offset R is of the wavelength order so that at $\lambda_0 = 630$ nm this accuracy is sufficient for fabrication of the waveguides of the described type. It should be stressed that the direct laser writing technique in the case of its applicability for fabrication of LPHFGs would make it possible to fabricate arrays of layered helical-core waveguides. In combination with a recently discovered possibility to integrate straight waveguides into a 3D photonic crystal [35], this could be used for developing unique methods of creating OVs arrays.

V. CONCLUSION

In this paper we have studied the possibility of changing the topological charge of incident beams by layered helical waveguiding structures that consist of planar layers. We have shown with the examples of Gaussian beam–optical vortex and optical vortex–optical vortex transformations that such structures can effectively change the topological charge of the incoming beam by unity, provided the resonance coupling conditions are fulfilled. We have solved the problems of the fundamental mode and optical vortex passage through a layered helical waveguide of a finite length. We have obtained the spectral characteristics of these processes and shown that such a waveguide can operate as a broadband generator of OVs from both regular and singular beams.

ACKNOWLEDGMENT

The authors are grateful to the reviewer for bringing to their attention the question of layered waveguide fabrication.

[1] M. Vasnetsov and K. Staliunas, in *Optical Vortices*, Vol. 228 of *Horizons of World Physics*, edited by M. Vasnetsov and K. Staliunas (Nova Science, Huntington, NY, 1999).

[2] M. S. Soskin and M. V. Vasnetsov, Prog. Opt. **42**, 219 (2001).

[3] S. H. Simpson and S. Hanna, J. Opt. Soc. Am. A **27**, 2061 (2010); O. V. Angelsky, A. P. Maksimyak, P. P. Maksimyak and S. G. Hanson, Ukr. J. Phys. Opt. **11**, 99 (2010); V. Garces-Chavez, K. Volke-Sepulveda, S. Chavez-Cerda, W. Sibbett, and K. Dholakia, Phys. Rev. A **66**, 063402 (2002); V. R. Daria, M. A. Go, and H.-A. Bachor, J. Opt. **13**, 044004 (2011); V. G. Shvedov, A. V. Rode, Y. V. Izdebskaya, A. S. Desyatnikov, W. Krolikowski, and Y. S. Kivshar, Phys. Rev. Lett. **105**, 118103 (2010).

[4] B. Spektor, A. Normatov, and J. Shamir, Appl. Opt. **47**, A78 (2008); J. Masajada, M. Leniec, and I. Augustyniak, J. Opt. **13** 035714 (2011); J. Masajada, M. Leniec, S. Drobczynski, H. Thienpont, and B. Kress, Opt. Express **17**, 16145 (2009); T. Brunet, J. -L. Thomas, and R. Marchiano, Phys. Rev. Lett. **105**, 034301 (2010).

[5] N. K. Metzger, M. Mazilu, L. Kelemen, P. Ormos, and K. Dholakia, J. Opt. **13** 044018 (2011).

[6] G. H. Lee, G. Foo, E. G. Johnson, and G. A. Swartzlander Jr., Phys. Rev. Lett. **97**, 053901 (2006); F. Tamburini, G. Anzolin, G. Umbriaco, A. Bianchini, and C. Barbieri, *ibid.* **97**, 163903 (2006); G. A. Shwartzlander Jr., E. L. Ford, R. S. Abdul-Malik, L. M. Close, M. A. Peters, D. M. Palacios, and D. W. Wilson, Opt. Express **16**, 10200 (2008).

[7] G. Gibson, J. Courtial, M. J. Padgett, M. Vasnetsov, V. Pas'ko, S. M. Barnett, and S. Franke-Arnold, Opt. Express **12**, 5448 (2004); Z. Bouchal and R. Chelechovsky, New J. Phys. **6**, 131 (2004); R. Čelechovský and Z. Bouchal, *ibid.* **9**, 328 (2007); J. A. Anguita, M. A. Neifeld, and B. V. Vasic, Appl. Opt. **47**, 2414 (2008).

[8] R. J. Voogd, M. Singh , S. Pereira , A. Van de Nes, and J. Braat, Proc. SPIE **5380**, 387 (2004); R. Pugatch, M. Shuker, O. Firstenberg, A. Ron, and N. Davidson, Phys. Rev. Lett. **98**, 203601 (2007); T. Wang, L. Zhao, L. Jiang, and S. F. Yelin, Phys. Rev. A **77**, 043815 (2008); L. E. Helseth, Opt. Lett. **36**, 987 (2011).

[9] M. W. Beijersbergen, L. Allen, H. E. L. O. van der Ween, and J. P. Woerdman, Opt. Commun. **96**, 123 (1993).

[10] M. W. Bejersbergen, R. P. C. Coerwinkel, M. Kristensen, and J. P. Woerdman, Opt. Commun. **112**, 321 (1994); X.-C. Yuan, J. Lin, J. Bu, and R. E. Burge, Opt. Express **16**, 13599 (2008).

[11] N. R. Heckenberg, R. McDuff, C. P. Smith, and A. G. White, Opt. Lett. **17**, 221 (1992).

[12] Y. J. Liu, X. W. Sun, D. Luo, and Z. Raszewsk, Appl. Phys. Lett. **92**, 101114 (2008); Ya. V. Izdebskaya, V. G. Shvedov, and A. V. Volyar, Opt. Lett. **30**, 2472 (2005); K. J. Webb and M.-C. Yang, Phys. Rev. E **74**, 016601 (2006); I. Skab, Y. J. Vasylkiv, V. Savaryn, and R. Vlokh, J. Opt. Soc. Am. A **28**, 633 (2011).

[13] D. McGloin, N. B. Simpson, and M. J. Padgett, Appl. Opt. **37**, 469 (1998); E. G. Johnson, J. Stack, and C. Kochler, J. Lightwave Technol. **19**, 753 (2001).

[14] C. D. Poole, C. D. Townsend, and K. T. Nelson, J. Lightwave Technol. **9**, 598 (1991).

[15] K. S. Lee and T. Erdogan, J. Opt. Soc. Am. A **18**, 1176 (2001).

[16] V. I. Kopp *et al.*, J. Opt. Soc. Am. B **24**, 48 (2007).

[17] C. N. Alexeyev, B. P. Lapin, and M. A. Yavorsky, Phys. Rev. A **78** 013813 (2008); C. N. Alexeyev and M. A. Yavorsky, J. Opt. A **10**, 085006 (2008).

[18] C. N. Alexeyev and M. A. Yavorsky, Phys. Rev. A **78**, 043828 (2008).

[19] A. Lakhtakia and R. Messier, *Sculptured Thin Films: Nanoengineered Morphology and Optics* (SPIE, Bellingham, WA, 2005).

[20] K. Robbie, M. J. Brett, and A. L. Lakhtakia, Nature (London) **384**, 616 (1996).
[21] Z. Y. Yang, M. Zhao, P. X. Lu, and Y. F. Lu, Opt. Lett. **35**, 2588 (2010).
[22] M. Thiel, H. Fischer, G. von Freymann, and M. Wegener, Opt. Lett. **35**, 166 (2010).
[23] K. K. Sheet, V. Mizeikis, S. Juodkazis, and H. Misawa, Appl. Phys. Lett. **88**, 221101 (2006).
[24] N. Wongkasem, C. Kamtongdee, A. Akyurtlu, and K. A. Mar, J. Opt. **12**, 075102 (2010).
[25] M. W. McCall, J. Opt. A **11**, 074006 (2009).
[26] A. W. Snyder and J. D. Love, *Optical Waveguide Theory* (Chapman and Hall, London, 1985).
[27] C. N. Alexeyev, A. V. Volyar, and M. A. Yavorsky, in *Lasers, Optics and Electro-Optics Research Trends*, edited by Lian I. Chen (Nova, New York, 2007), p. 131.
[28] C. N. Alexeyev, A. V. Volyar, and M. A. Yavorsky, J. Opt. A **10**, 015301 (2008).
[29] A. Yariv and P. Yeh, *Optical Waves in Crystals: Propagation and Control of Laser Radiation* (Wiley, New York, 1984); P. Yeh, J. Opt. Soc. Am. **69**, 742 (1979).
[30] Ya. Izdebskaya, V. Shvedov, and A. Volyar, J. Opt. Soc. Am. A **25**, 171 (2008); Ya. Izdebskaya *et al.*, Opt. Lett. **31**, 2523 (2006).
[31] S. Oh, K. R. Lee, U. -C. Paek, and Y. Chung, Opt. Lett. **29**, 1464 (2004).
[32] W. Shin, B.-A. Yu, Y. L. Lee, Y.-C. Noh, D.-K. Ko, and J. Lee, Opt. Fiber Technol. **14**, 323 (2008); O. V. Ivanov, Opt. Lett. **30**, 3290 (2005).
[33] G. Shvets, S. Trendafilov, V. Kopp, D. Neugroschl, and A. Z. Genack, J. Opt. A **11**, 074007 (2009).
[34] G. von Freymann, A. Ledermann, M. Thiel, I. Staude, S. Essig, K. Busch, and M. Wegener, Adv. Funct. Mater. **20**, 1038 (2010).
[35] I. Staude, G. von Freymann, S. Essig, K. Busch, and M. Wegener, Opt. Lett. **36**, 67 (2011).